Biochimica et Biophysica Acta 1818 (2012) 1–11

Contents lists available at SciVerse ScienceDirect

Biochimica et Biophysica Acta

journal homepage: www.elsevier.com/locate/bbamem

Substitution of a single amino acid residue in the aromatic/arginine selectivity filter alters the transport profiles of tonoplast aquaporin homologs ☆

Abul Kalam Azad [a,b,*], Naoki Yoshikawa [a], Takahiro Ishikawa [a], Yoshihiro Sawa [a], Hitoshi Shibata [a]

[a] Department of Life Science and Biotechnology, Faculty of Life and Environmental Science, Shimane University, 1060 Nishikawatsu, Matsue, Shimane 690-8504, Japan
[b] Department of Genetic Engineering & Biotechnology, Shahjalal University of Science and Technology, Sylhet 3114, Bangladesh

ARTICLE INFO

Article history:
Received 18 May 2011
Received in revised form 12 September 2011
Accepted 13 September 2011
Available online 22 September 2011

Keywords:
Aquaporin
ar/R selectivity filter
Transport selectivity
TgTIP
TIP homolog
Water channel activity

ABSTRACT

Aquaporins are integral membrane proteins that facilitate the transport of water and some small solutes across cellular membranes. X-ray crystallography of aquaporins indicates that four amino acids constitute an aromatic/arginine (ar/R) pore constriction known as the selectivity filter. On the basis of these four amino acids, tonoplast aquaporins called tonoplast intrinsic proteins (TIPs) are divided into three groups in *Arabidopsis*. Herein, we describe the characterization of two group I TIP1s (TgTIP1;1 and TgTIP1;2) from tulip (*Tulipa gesneriana*). TgTIP1;1 and TgTIP1;2 have a novel isoleucine in loop E (LE2 position) of the ar/R filter; the residue at LE2 is a valine in all group I TIPs from model plants. The homologs showed mercury-sensitive water channel activity in a fast kinetics swelling assay upon heterologous expression in *Pichia pastoris*. Heterologous expression of both homologs promoted the growth of *P. pastoris* on ammonium or urea as sole sources of nitrogen and decreased growth and survival in the presence of H_2O_2. TgTIP1;1- and TgTIP1;2-mediated H_2O_2 conductance was demonstrated further by a fluorescence assay. Substitutions in the ar/R selectivity filter of TgTIP1;1 showed that mutants that mimicked the ar/R constriction of group I TIPs could conduct the same substrates that were transported by wild-type TgTIP1;1. In contrast, mutants that mimicked group II TIPs showed no evidence of urea or H_2O_2 conductance. These results suggest that the amino acid residue at LE2 position is critical for the transport selectivity of the TIP homologs and group I TIPs might have a broader spectrum of substrate selectivity than group II TIPs.

1. Introduction

Aquaporins are integral membrane proteins that are involved in the transportation of water and other low molecular weight substances across biological membranes, and are found in all living organisms [1–2]. Whereas 13 different aquaporins have been identified in mammals [3], a greater diversity of aquaporins has been found in the genomes of plants. For examples, the genomes of rice (*Oryza sativa*), *Arabidopsis thaliana*, maize (*Zea mays*), and the poplar tree (*Populus trichocarpa*) contain 39, 35, 33, and 55 aquaporin homologs, respectively [4–8]. Plant aquaporins are generally classified into four subclasses on the basis of sequence homology and subcellular localization: (i) plasma membrane intrinsic proteins (PIPs), which are localized in the plasma membrane (PM); (ii) tonoplast intrinsic proteins (TIPs), which are localized in the vacuolar membranes (VM); (iii) nodulin-26-like intrinsic proteins; and (iv) small basic intrinsic proteins [9]. However, recently a fifth subclass of uncharacterized intrinsic proteins has been reported [8]. Plant aquaporins are involved in numerous physiological processes, such as cell elongation, adaptation and recovery from water deficit, anoxic stress, transpiration, photosynthesis, water uptake by roots, seed desiccation and germination, maintenance of cell turgor, inhibition of self-pollination, closure of leaf guard cells, and petal movement [9–16]. Functions of the aquaporins have also been associated with plant responses to numerous abiotic stresses, such as drought, osmotic stresses, and other perturbations in environmental conditions [17–18].

Recently, it has been reported that plant aquaporins are transporters not only of water but also of other substrates of physiological significance [2,9,19]. Among the plant aquaporins, TIPs are noted in particular for their ability to transport multiple substrates [20]. In addition to possessing water channel activity (WCA), certain TIPs from rice and tobacco have been reported to transport glycerol [21–22]. Urea conductance has been observed for several TIPs from *A. thaliana* (AtTIPs) [23–25]. The transport of NH_3, which is not substantially

Abbreviations: ar/R, aromatic/arginine; H_2DCFDA, 2,7-dichlorodihydrofluorescein diacetate; NPA, Asn-Pro-Ala; PIP, plasma membrane intrinsic protein; PM, plasma membrane; RACE, rapid amplification of cDNA ends; TIP, tonoplast intrinsic protein; TM, transmembrane; VM, vacuolar membranes; WCA, water channel activity; YNB, yeast nitrogen base

☆ "The nucleotide sequence data reported in this paper and deposited to DDBJ will appear in the DDBJ/EMBL/GenBank nucleotide sequence databases with the accession numbers AB591832 (TgTIP1;1) and AB591833 (TgTIP1;2)".

* Corresponding author at: Department of Genetic Engineering & Biotechnology, Shahjalal University of Science and Technology, Sylhet 3114, Bangladesh. Tel.: +88 0821 717850x411; fax: +88 0821 725050.
E-mail address: dakazad-btc@sust.edu (A.K. Azad).

0005-2736/$ – see front matter © 2011 Elsevier B.V. All rights reserved.
doi:10.1016/j.bbamem.2011.09.014

larger than water, has been reported for TIP homologs from wheat (TaTIP2;1, TaTIP2;2) [26–27] and *A. thaliana* (AtTIP2;1, AtTIP2;3 and AtTIP1;1) [28–29]. Two TIP homologs from *A. thaliana* (AtTIP1;1 and AtTIP1;2) have been shown to be permeable to H_2O_2 [30], whose size allows it to mimic water. However, although analysis of the genome of *A. thaliana* has revealed 10 putative TIPs [6], the functional activities of AtTIP2;2, AtTIP3;1, and AtTIP3;2 have not been reported to date. Moreover, the molecular mechanisms involved in the conduction of substrates through TIPs remain elusive.

Aquaporins comprise six transmembrane (TM) α-helices (helix H1–H6), which are connected by five loops (loops A–E), with both the N- and C-termini located on the cytoplasmic side of the membrane. They form tetrameric complexes in which each subunit behaves as a functional water channel [9]. The pore of the channel is characterized by two regions of constriction that specify the profile of transport selectivity. The first constriction is formed at the center of the pore by the close opposition of two asparagine residues, which are located in two Asn-Pro-Ala (NPA) motifs on loops B and E [31]. This constriction is involved in proton exclusion [32]. The second constriction is referred to as the aromatic/arginine (ar/R) constriction or the selectivity filter and is formed at the extracellular mouth of the pore by four residues from helix 2 (H2), helix 5 (H5), and loop E (LE1 and LE2), respectively [33–34]. Variability at this site is thought to form the basis of the broad spectrum of substrate conductance that is observed in plant aquaporins [5,8,31,35]. All the PIP homologs from plants that have been studied to date have ar/R selectivity filters that are similar to that of the water-specific mammalian aquaporin, AQP1. In contrast, TIPs show significant diversity within the ar/R region, which suggests that TIPs are more diverse in terms of transport function than PIPs [5,8,31,34]. On the basis of the four key residues in the ar/R selectivity filter, the 10 TIPs found in *A. thaliana* can be classified into three groups: i) group I (all AtTIP1s), ii) group II (all AtTIP2s, AtTIP3s, and AtTIP4;1), and iii) group III (AtTIP5;1) [31]. Group II has two subgroups, namely group IIa, which represents all AtTIP2s, and group IIb, which represents the AtTIP3s and AtTIP4;1. The 17 TIPs found in poplar also fit into these three groups [8]. To explore the mechanism by which NH_3/NH_4^+ and urea are conducted through TIPs, the ar/R site of AtPIP2;1 has been mutagenized to mimic the ar/R selectivity filter in TIPs from *A. thaliana* [29]. All mutants except the TIP2-like mutant conducted urea, but remained impermeable against NH_3/NH_4^+. Given that two native TIP homologs are known to allow ammonia conductance [29], it is clear that the understanding of the factors that dictate selectivity remains insufficient. Therefore, it would be of great value to explore the structure–function relationships of TIPs and the mechanism of selectivity toward different substrates further by mutagenizing the ar/R region of a TIP to mimic the ar/R selectivity filter of different TIP homologs from *A. thaliana* or other model plants.

Previously we have characterized four PIPs from the petals of tulip (*Tulipa gesneriana*) flowers, one of which was proposed to be associated with temperature-dependent and water transport-concomitant petal opening and closing movements [15–16]. TIPs with WCA might play a role in maintaining osmotic equilibrium within vacuoles during the fluctuations in cytosolic volume that may occur during tulip petal movement due to transcellular water transport. In the study reported herein, we have characterized two TIP1 homologs with WCA from tulip petals: TgTIP1;1 (DDBJ/EMBL/GenBank accession no. AB591832) and TgTIP1;2 (DDBJ/EMBL/GenBank accession no. AB591833). In both TgTIP1s, the ar/R selectivity filter had an Ile at the LE2 position, whereas a Val is found at this position in all TIP1 homologs from *A. thaliana*, rice, maize, and poplar [5,8,31]. To investigate this intriguing characteristic of the TgTIP1 homologs, and to mimic the ar/R regions of group I and II TIPs from *A thaliana*, the Ile at LE2 and Ala at LE1 in TgTIP1;1 were mutated and the resulting mutant proteins heterologously expressed in *Pichia pastoris*. The conduction of water, NH_3/NH_4^+, urea, and H_2O_2 by these wild-type and mutant TIP homologs was then studied. The wild-type and mutant TIP homologs showed different transport selectivities and these differences were linked to amino acid substitutions at the LE2 position of the ar/R selectivity filter.

2. Materials and methods

2.1. RNA extraction and cDNA synthesis

Total RNA extracted from the petals of two-day-old tulip (*T. gesneriana*) flowers was used to synthesize first strand cDNA for the isolation of full-length cDNA using methods described previously [16].

2.2. Isolation of gene sequences encoding TIPs

Degenerate primers (forward primer, 5′-TCTACATCATCGCCCAGCTCCTC-3′; reverse primer, 5′-CGTACACAATCCCCGCGATTCCT-3′) were designed using conserved sequences of TIP genes in *A. thaliana*, maize and other plant species. PCR was performed with the cDNA as the template using *Taq* polymerase (TaKaRa Bio, Japan) as described previously [16]. The amplified PCR products were cloned into the pT7Blue T-vector (Novagen, Germany), and then sequenced using an ABI Prism™ 3100-Avant Genetic Analyzer (Applied Biosystems, USA). This sequence information was used to design gene-specific primers (Table 1) for use in the rapid amplification of cDNA ends (RACE) technique to obtain full-length cDNA as described previously [16].

2.3. Construction of TgTIP1;1-G_3-H_6, TgTIP1;2-G_3-H_6, and the mutants of TgTIP1;1-G_3-H_6 and heterologous expression in P. pastoris

Constructs that encoded TgTIP1;1 (TgTIP1;1-G_3-H_6) and TgTIP1;2 (TgTIP1;2-G_3-H_6) with a $(Gly)_3$-$(His)_6$ tag before the stop codon were synthesized using the pPICZ-B expression vector (Invitrogen, USA), transformed into *P. pastoris* strain KM71H (Invitrogen, USA), and heterologously expressed as described previously [36]. Prior to yeast transformation, the TgTIP1;1-G_3-H_6/pPICZ-B and TgTIP1;2-G_3-H_6/pPICZ-B plasmids were linearized with *Pme* I (New England BioLabs Inc., USA). The empty plasmid pPICZ-B, without any expression cassette, was also transformed into the same *P. pastoris* strain. Three single mutants (I201V, I201R, and A195G) and a double mutant (A195G/I201R) of TgTIP1;1-G_3-H_6 were constructed by site-directed mutagenesis as described previously [16] and transformed into the same *P. pastoris* strain. Transformants were selected by plating on YPDS agar (1% yeast extract, 2% peptone, 2% dextrose, 1 M sorbitol, and 2% agar) that contained 100 μg/ml zeocin. Integration of the gene of interest into the *P. pastoris* genome was verified by PCR using genomic DNA isolated from the transformants, in accordance with the manufacturer's instructions (Invitrogen, USA). Yeast culture, induction of protein expression, and harvesting of cells were performed in accordance with Daniels and Yeager [36]. The cell pellets were frozen and stored at −80 °C until required.

Table 1
List of primers used for RACE.

Primers	Sequence	Use
3R-TIP1;1	5′- GGCACCGGCACCTTCGGTCTCGT-3′	TIP1;1 3′ RACE
3R-TIP1;2	5′- GGTCTCGTCGCCGGCGTCAGCGT-3′	TIP1;2 3′ RACE
5R-TIP1;1	5′- CTTTCCGCCATCAACCTAGCCAAAAATCAC-3′	TIP1;1 5′ RACE
5R-TIP1;2	5′- GACCGGCATAGTTTGGGGTTGCATTGTG-3′	TIP1;2 5′ RACE
GeneRacer 3′	5′-GCTGTCAACGATACGCTACGTAACG-3′	3′ RACE
GeneRacer 5′	5′-CGACTGGAGCACGAGGACACTGA-3′	5′ RACE

2.4. Membrane vesicles preparation and Western immunoblotting

Cultures of the transformed *P. pastoris* expressing recombinant aquaporins were centrifuged at 1500 *g* for 5 min to harvest the cells. The total membrane vesicles were prepared as demonstrated by Azad et al. [37]. The PM and the VM vesicles prepared as described by Tamas et al. [38] and Nakanishi et al. [39], respectively were used for Western analysis as demonstrated previously [37].

2.5. Spheroplast swelling assay for WCA

Spheroplasts were prepared as described previously [37] from yeasts transformed with empty pPICZ-B or pPICZ-B containing constructs for the TIP homologs or TgPIP2;2-G_3-H_6 [16,37]. The spheroplasts were washed once and resuspended finally in 100 mM potassium phosphate, pH 7.0 that contained 1 mM EDTA and 2.0 M sorbitol at an A_{475} of 3.0. Spheroplasts were shocked hypo-osmotically by mixing with an equal volume of 100 mM potassium phosphate, pH 7.0 that contained 1 mM EDTA. The kinetics of spheroplast swelling and volume changes at 475 nm and 10 °C were recorded as described previously [30] by using a temperature-controlled rapid-scan stopped-flow spectroscopy system (RSP-1000, UNISOKU, Japan). To investigate the inhibition by Hg^{+2}, which is a well-known aquaporin inhibitor [40], the spheroplasts were pretreated with 2 mM $HgCl_2$ for 10 min before hypo-osmotic shock. The $HgCl_2$ solution was prepared in 100 mM potassium phosphate, pH 7.0, supplemented with 2.0 M sorbitol. All data presented are averages of at least 10 trace recordings. The rate constant of the decrease of scattered light intensity is proportional to the water permeability coefficient [41–42]. Rate constants were calculated by fitting the curves with single exponential functions as described previously [43].

2.6. Growth analysis

For growth assays, *P. pastoris* expressing recombinant aquaporins or containing empty pPICZ-B were grown in BMMY [1% yeast extract, 2% peptone, 1.34% YNB (yeast nitrogen base), 4×10^{-5}% biotin, 1% methanol in 100 mM potassium phosphate, pH 6.0] medium for 30 h. Cells were harvested as described above and resuspended in YNB medium (1.34% YNB in 100 mM potassium phosphate, pH 6.0) to an OD_{600} of 1.0, and then diluted in a 10-fold dilution series down to $1/10^6$. Aliquots (5 μl) from the last consecutive dilutions ($1/10^3$ to $1/10^6$) were spotted onto the various types of agar plate described below. To investigate NH_3/NH_4^+ and urea transportation, cells were spotted on YNB agar (1.34% YNB, 2% dextrose, 4×10^{-5}% biotin, 100 mM potassium phosphate, pH 7.0) supplemented either with NH_4Cl or urea as the sole nitrogen source. To examine the effects of H_2O_2 and osmotica on growth, cells were spotted on YPD agar media (1% yeast extract, 2% peptone, 2% dextrose, 1.34% YNB, 4×10^{-5}% biotin, 100 mM potassium phosphate, pH 6.0) supplemented with H_2O_2 or sorbitol. The cells were incubated at 30 °C and growth was monitored, with photographs taken after identical incubation periods over the course of 2–3 days. For viable cell counts, 5 μl aliquot from the last consecutive dilutions ($1/10^3$ to $1/10^6$) plus 95 μl in 100 mM potassium phosphate buffer, pH 6.0, were spread on agar media used to investigate the transport of NH_3/NH_4^+ and urea or the effects of H_2O_2 and osmotica on growth. The viable cell count was performed manually using five independent experiments with four replicates of each.

2.7. Fluorescence assay

Each transformant was grown in 5 ml of BMMY media for 30 h at 30 °C on a shaker at 230 rpm. The cells were then harvested by centrifugation at 1500 *g* for 5 min and the supernatant was decanted. Cells were resuspended in phosphate-buffered saline (PBS) and adjusted to $OD_{600}=2.0$. Aliquots of 2 ml of the resuspended cell suspensions were supplemented with the oxidant-sensitive fluorescent dye H_2DCFDA (2,7-dichlorodihydrofluorescein diacetate; Molecular Probes, USA) at a final concentration of 10 μM and then incubated at 30 °C and 230 rpm for 1 h to allow the cells to take up the dye. Cells were then washed five times with PBS and finally resuspended in PBS at $OD_{600}=1.5$. The fluorescence was measured before the addition of H_2O_2 (final concentration of 5 mM) and afterwards at 10 min intervals using a VersaFluor™ Fluorometer System (Bio-Rad, USA) with a 490/10 excitation filter (485–495 nm) and a 520/10 emission filter (515–525 nm). To examine the effect of Hg^{+2}, cells were pretreated for 10 min with 2 mM $HgCl_2$ before the addition of H_2O_2.

2.8. Homology modeling

Homology models were constructed using the Molecular Operating Environment software (MOE 2009.10; Chemical Computing Group, Quebec, Canada). The sequences of the TIP homologs were aligned with the open conformation of SoPIP2;1 [44] [Protein Data Bank (PDB) code, 2B5F] using the MOE multiple sequence and structural alignment algorithm, with the structural alignment tool and the BLOSUM62 substitution matrix. The alignment of the TIP sequences was based on both sequence and structural homology with the experimentally derived structure of SoPIP2;1. 3D structural models were formed using the MOE homology program, and was based on a segment matching procedure and a best intermediate algorithm, with the option to refine each individual structure enabled. A database of 10 structures, each of which was individually refined to a root-mean-square (RMS) gradient of 1 Å, was generated and the best one was chosen as the crude template for further refinement. Comparative analysis of this database of structures showed that most deviations were on the periplasmic side and that the TM α-helices and NPA motifs were superimposible. The stereochemical quality of the models was assessed by structural analysis using the Protein Report Function of the MOE Protein Structure Evaluation, which searches for disallowed bond angles, bond lengths and side chain rotamers. Those models were then subjected to energy minimization until the RMS gradient became 0.01. The model that best matched these criteria was selected for further use in all structural analyses.

2.9. Statistical analysis

For statistical analysis, Student's *t* test was used. $P<0.05$ was considered to be statistically significant. Data are presented as the means ± standard errors of the means (SEM), or as noted in the figure legends.

3. Results

3.1. Characterization of TIP genes from tulip petals

PCR amplification of cDNA from tulip petals using primers against conserved regions of TIP genes, followed by cloning, sequencing, and 3′- and 5′-RACE, enabled us to identify two genes that showed homology to TIPs from other plants (Fig. 1). On the basis of the deduced amino acid sequences, the two TIPs were classified as belonging to the TIP1 subclass and named TgTIP1;1 and TgTIP1;2 in accordance with the suggested nomenclature for TIPs in plants [7]. The deduced amino acid sequences for both TgTIP1;1 and TgTIP1;2 were 250 amino acids, with predicted molecular masses for the proteins of 25,440 and 25,293 Da, respectively.

The amino acid sequences of TgTIP1;1 and TgTIP1;2 were typical of aquaporins (Fig. 1) and the secondary structures of the proteins were predicted using SOSUI (http://bp.nuap.nagoya-u.ac.jp/sosui/), TMpred (http://www.ch.embnet.org/software/TMPRED_form.html), and the tools of ExPASy (http://kr.expasy.org/tools/). The proteins

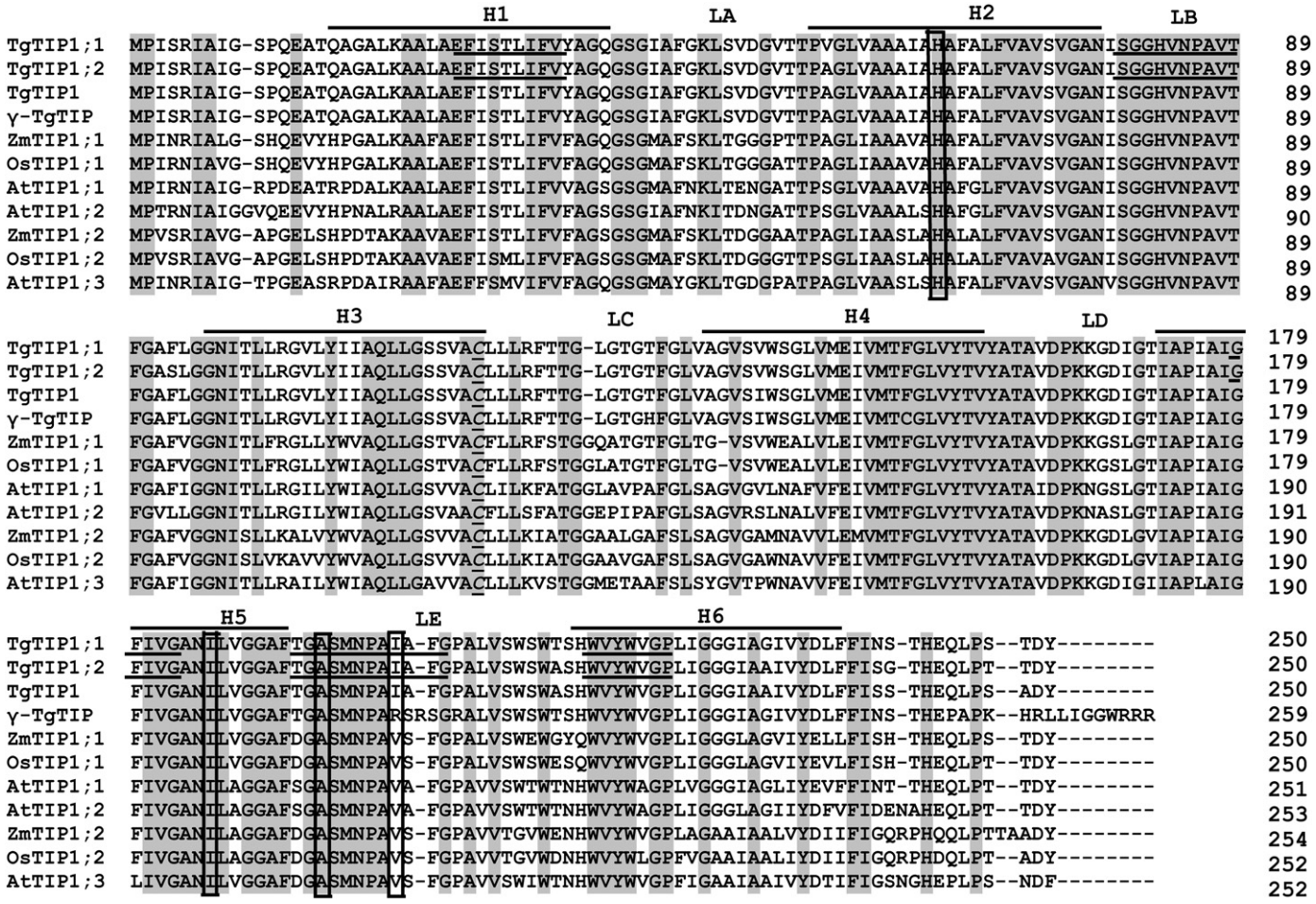

Fig. 1. Alignment of the deduced amino acid sequences of TgTIP1;1 and TgTIP1;2, and comparison with TgTIP1 (Accession No. FJ234420), γ-TgTIP (X95650), AtTIP1;1 (NM_129238), AtTIP1;2 (NM_113559), AtTIP1;3 (NM_116377), ZmTIP1;1 (AF037061), ZmTIP1;2 (AF326500), OsTIP1;1 (P50156), and OsTIP1;2 (Q94CS9). Amino acids that are conserved in these sequences are highlighted in gray. The six TM α-helices, H1–H6, are indicated with a bar and the connecting loops are labeled LA–LE. The two highly conserved NPA motifs are located in loops B and E and the consensus regions in all TIPs are underlined. The four key residues in the ar/R selectivity filter (Fig. 3) are boxed. In H3, the conserved Cys (italicized and underlined) in all TIP1 homologs was identified as the mercury-sensitive site [60].

featured six hydrophobic TM α-helices, five loops, and two NPA signature motifs in loops B and E. Similar to all TIPs from *A. thaliana*, maize, and rice, TgTIP1;1 and TgTIP1;2 contained the consensus regions that are indicated in Fig. 1. TBLASTN (http://blast.ncbi.nlm.nih.gov/Blast.cgi) analysis of the deduced amino acid sequences of TgTIP1;1 and TgTIP1;2 indicated that they shared 96–98% amino acid identity with two TIPs from tulip: TIP1 (EMBL/GenBank/DDBJ accession no. FJ234420) and γ-TIP [45], and we showed them as TgTIP1 and γ-TgTIP, respectively (Figs. 1 and 2). TgTIP1;1 and TgTIP1;2 shared 97.2% amino acid identity, and had 76–79% amino acid identity to other TIP1s from *A. thaliana*, maize, rice, and poplar. A phylogenetic analysis of TgTIPs including all TIPs from *A. thaliana* and maize confirmed that TgTIP1;1 and TgTIP1;2 clustered with TIP1s and resembled TgTIP1 and γ-TgTIP most closely (Fig. 2). Structural homology models of TgTIP1;1 and TgTIP1;2, which were based on the 3D structure of SoPIP2;1 [44], showed two pore constrictions in the water channel (Fig. 3; only TgTIP1;1 is shown). One of these constrictions was formed by the opposing NPA motifs found in loops B and E. The second constriction, the ar/R constriction, was formed in TgTIP1;1 and TgTIP1;2 by His-65 (in H2), Ile-186 (in H5), Ala-195 (at LE1), and Ile-201 (at LE2) (Fig. 3B; only TgTIP1;1 is shown). Although all the TIP homologs of *A. thaliana*, maize, rice, and poplar in group I have Val at LE2 [5,8,31], TgTIP1;1, TgTIP1;2, and TgTIP1 all featured an Ile at this position. The γ-TgTIP has an Arg in the corresponding position although it clustered with TIP1s. The 3D models of TgTIP1;1 and TgTIP1;2 superposed separately onto that of AtTIP1;1 revealed that I201 of the both homologs (only TgTIP1;1 is shown) projected into the pore and narrowed it slightly (Fig. 3B). These results indicate that the ar/R selectivity filter in TIP homologs might be more divergent in other plants than in model plants.

3.2. Expression and WCA of TIP homologs in *P. pastoris*

To mimic the ar/R constrictions of all the TIP homologs in groups I and II from *A. thaliana* [31], we constructed three single mutants and a double mutant of the recombinant TgTIP1;1-G_3-H_6 (henceforth TgTIP1;1), which were designated I201V, I201R, A195G, and A195G/I201R, respectively (Table 2). The I201V mutant was designed to mimic the ar/R constriction site of AtTIP1 (group 1), A195G/I201R to mimic that of AtTIP2 (group IIa), and I201R to mimic those of the AtTIP3 and AtTIP4;1 (group IIb) homologs. The heterologous expression of TgTIP1;1 and its mutants, together with that of TgTIP1;2-G_3-H_6 (hereafter TgTIP1;2), were verified by Western blot analysis using an anti-His (C-terminal) antibody, which reacted specifically with proteins that contained a C-terminal polyhistidine tag (His_6). Fig. 4A shows that TgTIP1;1 and its mutants and TgTIP1;2 were present in the VM vesicles of yeast cells as a band of approximately 26 kDa, as expected for their monomeric forms. In contrast, the positive control TgPIP2;2-G_3-H_6 (henceforth TgPIP2;2), which has WCA in *Xenopus* oocytes and *P. pastoris* [16, 37], appeared in the PM vesicles as a band of ~31 kDa (Fig. 4A).

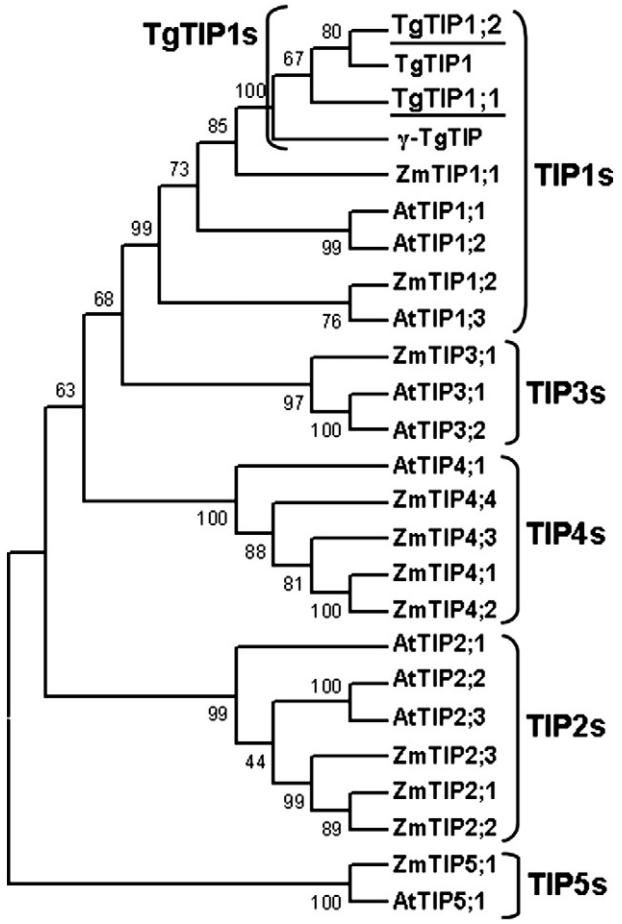

Fig. 2. Phylogenetic tree of TIPs from *A. thaliana*, maize, and tulip (TgTIPs). The deduced amino acid sequences of TIP-encoding genes were aligned using the ClustalW computer program (http://clustalw.ddbj.nig.ac.jp/top-e.html) and a phylogenetic tree was constructed using Molecular Evolution Genetic Analysis (MEGA), version 4.0 [61]. The evolutionary history was inferred using the Neighbor-Joining method. The percentage of replicate trees in which the associated taxa clustered together in the bootstrap test (1000 replicates) are shown next to the branches and the genetic distance was estimated by the p-distance method. The tulip TIPs that we characterized are underlined. The accession numbers of the TIPs of *A. thaliana* (AtTIPs) and maize (ZmTIPs) were reported by Johanson et al. [6] and Chaumont et al. [7], respectively, and those of TgTIP1 and γ-TgTIP were mentioned in Fig. 1.

The functional WCA of heterologous TIPs expressed in *P. pastoris* was investigated by assessing spheroplast swelling and growth. In the spheroplast swelling assays, the swelling of spheroplasts that expressed the heterologous aquaporins and that of spheroplasts that harbored the empty pPICZ-B vector were monitored after hypo-osmotic shock and compared (Fig. 4B). Heterologous expression of TgTIP1;1, TgTIP1;2, and the positive control, TgPIP2;2, resulted in a rapid drop in light scattering after hypo-osmotic shock, which indicated swelling of the spheroplasts due to an increasing influx of water. Fig. 4B shows that spheroplasts that expressed TgTIP1;1 or TgTIP1;2 had higher WCA than those that expressed TgPIP2;2. The treatment of the spheroplasts with $HgCl_2$, which is an aquaporin inhibitor, increased the relative light scattering of all spheroplasts that expressed the heterologous aquaporins. Following mercury treatment, the light scattering curves generated by the spheroplasts that expressed TgTIP1;1 or TgTIP1;2 were identical (only that of TgTIP1;1 is shown), but these spheroplasts showed a higher water flux than spheroplasts that contained the empty pPICZ-B vector. This might be due to incomplete inhibition of the aquaporins due to an insufficient period of preincubation with mercury. With the present assay approach, the increase in light scattering of the spheroplasts that contained the empty pPICZ-B vector after mercury treatment indicated that the native aquaporin of *P. pastoris* has WCA [46] and is mercury sensitive. On the basis of the swelling kinetics, the rate constants (k) for all spheroplasts that expressed the TgTIP1;1 mutants were compared with those that expressed the wild-type TgTIP1;1 or contained the empty pPICZ-B vector (Fig. 4C). Spheroplasts that expressed the I201V mutant displayed a significantly higher k than those that expressed the wild-type protein, whereas those that expressed the A195G mutant exhibited almost the same k as observed for the wild type. In contrast, the I201R and A195G/I201R mutants both showed a lower k than the spheroplasts that expressed wild-type TgTIP1;1. However, following Hg^{+2} pretreatment, k was almost identical in spheroplasts that expressed wild-type TgTIP1;1 or the mutant proteins. Together these results suggest that all of the TIP homologs investigated in this study had mercury-sensitive WCA and that the rate of water transportation was highest in the I201V mutant, which was designed to mimic group I TIPs of *A. thaliana*.

The WCA of the TIP homologs was monitored further using a phenotypic growth assay in YPD agar supplemented with or without sorbitol (Fig. 4D). The growth of *P. pastoris* transformed with empty pPICZ-B or the pPICZ-B containing constructs for the TIP homologs and TgPIP2;2 could not be distinguished on YPD plates that were not supplemented with sorbitol (conditions that do not induce stress). When exposed to hyperosmotic stress by the addition of 1.5 M sorbitol to the growth medium, cells that expressed the TIP homologs or TgPIP2;2 showed reduced growth compared to that in medium without sorbitol. In contrast, the growth of cells that contained the empty pPICZ-B vector did not change significantly upon exposure to the same hyperosmotic stress with sorbitol. Although the growth assay had been done with different concentrations of sorbitol (0.5, 1.0 and 1.5 M), only the results observed with the supplementation of 1.5 M sorbitol was shown, as the phenotypes at this hyperosmotic condition could be easily distinguished between cells that expressed recombinant aquaporins and cells that contained the empty pPICZ-B. This result indicates that expression of the heterologous TIP homologs confers water channel-mediated osmosensitivity upon the cells.

3.3. Amino acid substitution at the LE2 position in the ar/R constriction changes the substrate selectivity

To investigate the conductance of NH_3/NH_4^+ and urea by the TIP homologs, we used a phenotypic growth assay. Yeast that contained the empty vector could not be distinguished clearly from those that expressed the heterologous TIP homologs when grown on YNB plates supplemented with either ammonium or urea at a concentration of 1 mM or less as the sole nitrogen source (Fig. 5, data with less than 1 mM ammonium and those with 1 mM or less urea or those with no ammonium or urea supplementation are not shown). However, all cells that expressed the TIP homologs grew better than those transformed with the empty pPICZ-B vector on YNB plates supplemented with 2 mM ammonium. The enhanced growth of the cells that expressed the TIP homologs was presumed to be due to increased uptake of ammonium as an external nitrogen source from the medium. This enhancement of growth was less evident in yeast that expressed the I201R mutant than in cells that expressed the other TIP homologs. When 2 mM urea was added as the sole source of nitrogen to the YNB medium, the growth of yeast that expressed wild-type TgTIP1s, the I201V mutant or the A195G mutant was enhanced significantly compared with that of yeast that harbored the empty vector. Yeast that expressed the I201R or A195G/I201R mutant did not show the same enhanced growth, but grew at a similar rate to yeast transformed with the empty vector. The increased growth of cells that expressed the wild-type TgTIP1s and mutants I201V and A195G was presumed to be due to increased uptake of urea as an external source of nitrogen from the medium. These data indicated that heterologous expression of the TIP homologs facilitated the uptake of

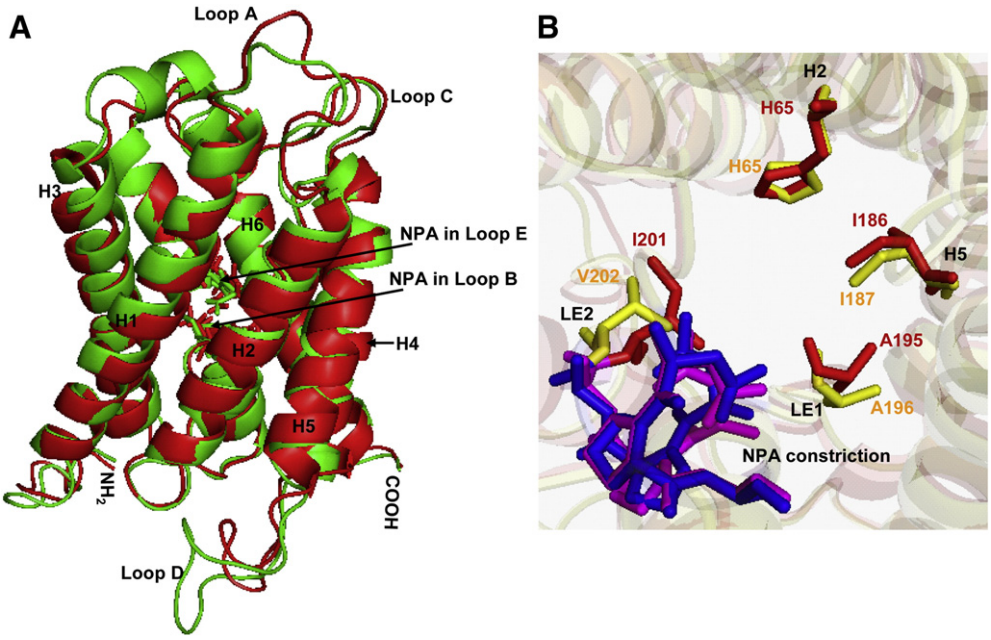

Fig. 3. Homology modeling of TgTIP1;1. SoPIP2;1 of spinach (PDB code, 2B5F; green) and the 3D model of TgTIP1;1 (red) were superposed (A; side view). The NPA motifs (shown as sticks) in loops B and E are indicated by arrows. The TM α-helices and loops are indicated. The ar/R selectivity filter of TgTIP1;1 (red) is superposed on that of AtTIP1;1 (yellow) from *A. thaliana* (B), as seen from the extracellular aspect along the axis of the pore. The 3D models of TgTIP1;1 and AtTIP1;1 were constructed first separately with SoPIP2;1 and then superposed. The residues that form the ar/R tetrad in the superposed structures are shown as sticks. The residues of TgTIP1;1 are shown in red and those of AtTIP1;1 in yellow. The TM α-helices and the loops to which these residues belong are indicated. The NPA constriction formed in TgTIP1;1 (magenta sticks) and superposed on AtTIP1;1 (blue sticks) is shown (B).

ammonium from the medium in a TIP homolog-independent manner and the uptake of urea in a TIP homolog-specific manner.

We then used phenotypic growth assays and fluorescence techniques similar to those used previously to study H_2O_2 conductance in plant aquaporins to examine the H_2O_2 conductance of the TIP homologs [30,47]. The growth of yeast that expressed some of the TIP homologs was found to be affected by H_2O_2 in a dose–dependent manner, whereas yeast that contained the empty vector was almost insensitive to 2 mM H_2O_2 in YPD medium. Therefore, only the results observed with 2 mM H_2O_2 are shown (Fig. 6A). Yeast that expressed heterologously the wild-type TgTIP1s and the I201V mutant showed markedly reduced growth and survival on medium that contained H_2O_2 (Fig. 6A). Yeast that expressed the A195G mutant also showed increased sensitivity to H_2O_2 supplied externally, albeit to a lesser extent. In contrast, cells that expressed the I201R and A195G/I201R mutants remained insensitive to H_2O_2 in the medium, in a similar manner to yeast that contained the empty pPICZ-B vector. Growth and survival of yeasts that expressed the wild-type TgTIP1s or the I201V mutant were repressed even with 0.75 mM H_2O_2 in the media compared with the yeast containing the empty vector control (data not shown). To investigate whether heterologous expression of the TIP homologs resulted in a decreased scavenging capacity of the yeast cells, we measured catalase activity using methods described previously [30]. No significant change in catalase activity was observed in the cells that expressed the TIP homologs or were transformed with the empty vector (data not shown). Therefore, the reduced growth of cells that expressed the wild-type TgTIP1s or the I201V or A195G mutant was due to increased oxidative stress, which in turn resulted from increased uptake of H_2O_2 from the medium.

Table 2
Constructs to mimic the ar/R constriction of the TIP homologs of *Arabidopsis thaliana*.

Construct	Amino acids in the ar/R constriction				Mimicked TIPs of *A. thaliana*	Group[a]
	H2	H5	LE1	LE2		
I201V	H	I	A	V	AtTIP1;1	I
	H	I	A	V	AtTIP1;2	
	H	I	A	V	AtTIP1;3	
A195G/I201R	H	I	G	R	AtTIP2;1	IIa
	H	I	G	R	AtTIP2;2	
	H	I	G	R	AtTIP2;3	
I201R	H	I	A	R	AtTIP3;1	IIb
	H	I	A	R	AtTIP3;2	
	H	I	A	R	AtTIP4;1	

[a] Groups have been proposed by Wallace and Roberts [31].

To investigate whether the increased growth sensitivity of yeast that expressed the heterologous TIP homologs was due to H_2O_2 influx, we detected intracellular H_2O_2 using an oxidant-sensitive fluorescent dye H_2DCFDA, which can enter the cytosol by passive diffusion. Following diffusion into the cytosol, the esters of H_2DCFDA are cleaved by endogenous esterase, which makes it impermeable to the membrane and susceptible to oxidation by reactive oxygen species, such as H_2O_2, and results in an increase in fluorescence [47]. The uptake of H_2O_2, as measured by this fluorescent assay, was highest in yeast cells that expressed the I201V mutant (Fig. 6B). Upon exposure to H_2O_2, cells that expressed the A195G mutant showed slightly lower fluorescence than cells that expressed wild-type TgTIP1s. Pretreatment of cells with $HgCl_2$ prior to exposure to H_2O_2 inhibited the accumulation of H_2O_2 significantly in cells that expressed wild-type TgTIP1s or the I201V or A195G mutant. In contrast, the fluorescence was not significantly different in cells that expressed the I201R or A195G/I201R mutant, with or without mercury pretreatment, as compared with cells transformed with the empty vector alone. After the addition of H_2O_2 to cells that expressed TgTIP1s or the I201V or A195G mutant, the cells were harvested by centrifugation. No fluorescence was detected in the supernatant, which confirmed that the increase in fluorescence observed was due to increased uptake of H_2O_2 by these cells.

Because the contrast was too high to distinguish the differences in growth, particularly, at cell concentrations of 10^{-3} and 10^{-4} dilutions (Figs. 4D, 5 and 6A), we further determined the viable cell

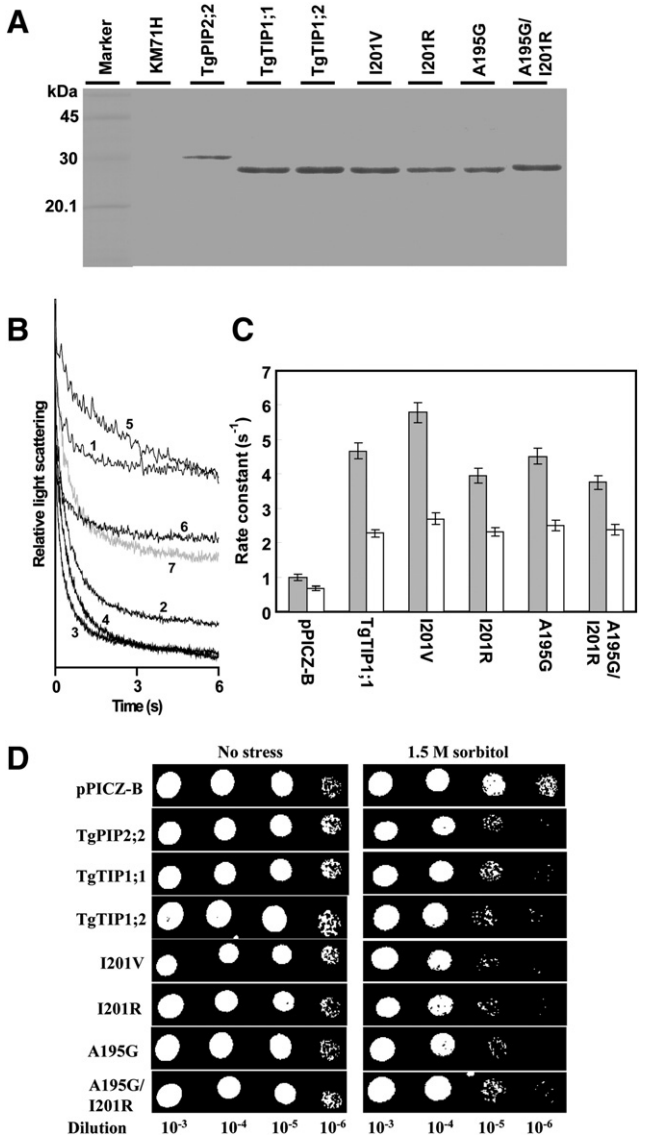

Fig. 4. Aquaporin-mediated osmotic water transport. (A) Expression of TgPIP2;2 in the PM and that of TgTIP1;1, TgTIP1;2, or the TgTIP1;1 mutants I201V, I201R, A195G and A195G/I201R in the VM of *P. pastoris* was determined by Western blotting. (B, C) Spheroplasts were prepared from 30 h cultures of *P. pastoris* KM71H that expressed the recombinant aquaporins or that harbored the empty pPICZ-B vector. The spheroplasts were resuspended in 100 mM potassium phosphate, pH 7.0 that contained 1 mM EDTA and 2.0 M sorbitol at an A_{475} of 3.0. The spheroplasts were then mixed in a fast kinetic stopped-flow apparatus with the same buffer without sorbitol at 10 °C. A time course of the changes in the 90° scattered light intensity was measured at 475 nm. The kinetics for mercury-untreated spheroplasts transformed with pPICZ-B (1), TgPIP2;2 as a positive control (2), TgTIP1;1 (3), or TgTIP1;2 (4) and that for mercury-treated spheroplasts transformed with pPICZ-B (5), TgPIP2;2 (6) or TgTIP1;1 (7) are shown in B. The data presented are averages of at least 10 trace recordings each taken over a period of 6 s. The rate constant (k, in s^{-1}) following mercury treatment (open bar) or without mercury treatment (solid bar) was calculated on the basis of the swelling kinetics in 1 s and shown in C. (D) Expression of TIP homologs in *P. pastoris* caused growth defects under hyperosmotic conditions. Aliquots (5 μl) of 10^{-3} to 10^{-6} dilutions of resuspended cells spotted onto YPD agar plates supplemented without (no stress) or with 1.5 M sorbitol are shown. Data shown are representative of three independent experiments.

counts for the experiments corresponding to Figs. 4D, 5 and 6A. Table 3 showed that the viable cell counts correlated with the pattern of growth under different conditions. However, due to dense growth, viable cell counts at cell concentration of 10^{-3} dilution are not shown.

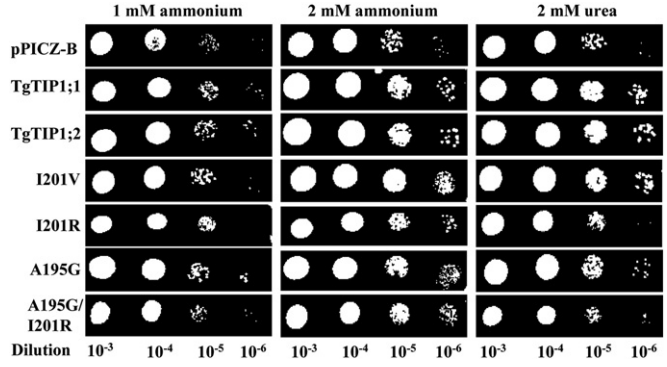

Fig. 5. Growth assay of TIP homologs-expressing *P. pastoris* on the media containing ammonium and urea. Aliquots (5 μl) of 10^{-3} to 10^{-6} dilutions of resuspended cells were spotted onto YNB agar plates supplemented with the indicated concentrations of either ammonium or urea as sole nitrogen sources. Data shown are typical of four separate experiments with consistent results.

3.4. Pore conformation might be changed by amino acid substitution at the LE2 position in the ar/R selectivity filter

In the ar/R selectivity filter, although the His in H2 and Ile in H5 are conserved in all TIPs in groups I and II, substitutions are observed at the LE1 and LE2 positions (Table 2; [31]). The Ala at LE1 that is conserved in TIP homologs in groups I and IIb is substituted by a small, flexible Gly residue in TIPs of group IIa. Val, which is conserved at LE2 in all TIPs in group I, is substituted by Arg in all TIPs in group II. The differences in pore structures that were imparted by varying the residue at the LE2 position were apparent from the comparison

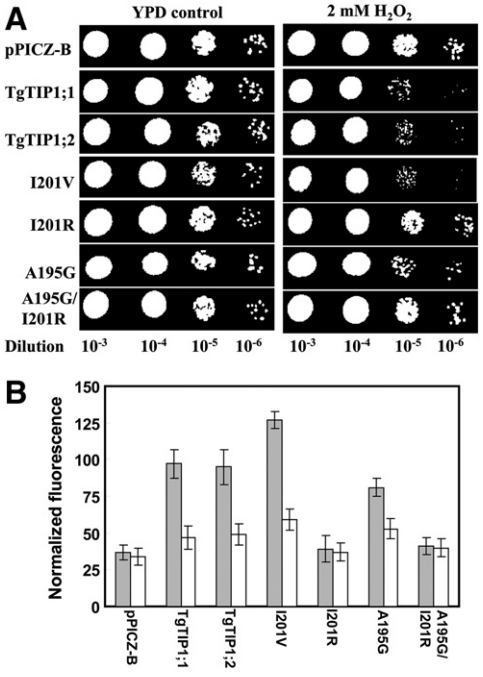

Fig. 6. Growth and survival of *P. pastoris* on the media that contained H_2O_2. (A) Aliquots (5 μl) of 10^{-3} to 10^{-6} dilutions of resuspended cells were spotted onto YPD medium supplemented without (YPD control) or with 2 mM H_2O_2. Data were reproducible in at least three independent experiments. (B) H_2O_2 levels in *P. pastoris* that expressed the TIP homologs. Cells transformed with TIP homologs or pPICZ-B empty vector were grown for 30 h and preincubated with H_2DCFDA. The fluorescence was recorded at 10 min intervals (20 readings min^{-1}) and the normalized fluorescence detected 30 min after application of 5 mM H_2O_2 is shown. Solid and open bars represent the normalized fluorescence of Hg^{+2}-untreated and Hg^{+2}-treated cells, respectively. The data shown are the means ± SEM of five independent experiments.

Table 3
Viable cell counts of TIP homologs-expressing *P. pastoris* grown on YPD agar media supplemented either with 1.5 M sorbitol or 2 mM H_2O_2 and YNB agar media supplemented either with ammonium or urea.

Tranformants	Viable counts (CFU/μl) on [a,b]											
	YPD agar containing 1.5 mM sorbitol			YNB agar containing 2 mM NH_4^+			YNB agar containing 2 mM urea			YPD agar containing 2 mM H_2O_2		
	10^{-4}	10^{-5}	10^{-6}	10^{-4}	10^{-5}	10^{-6}	10^{-4}	10^{-5}	10^{-6}	10^{-4}	10^{-5}	10^{-6}
pPICZ-B	647	68	7	197	22	2	191	18	1	625	63	6
TgTIP1;1	164	17	2	447	43	4	398	38	4	124	12	1
TgTIP1;2	172	18	2	452	44	4	428	41	4	126	13	1
I201V	126	14	1	489	48	5	456	43	4	108	11	1
I201R	208	19	1	327	32	3	186	17	1	583	56	5
A195G	161	15	1	448	42	4	367	34	3	154	16	2
A195G/I201R	229	21	2	442	42	4	179	19	1	601	58	5

[a] The number of CFU is the mean of five independent experiments with four replicates of each showing the similar results.
[b] 10^{-4}, 10^{-5} and 10^{-6} indicate the last consecutive dilutions used in Figs. 4D, 5 and 6A.

of homology models of the wild-type TgTIP1;1 and its mutants (Fig. 7). Although the overall topology of the models of the TIP homologs was similar to the SoPIP2;1 structural template, the pore structures, as well as the pore apertures, differed significantly. A Val residue at position LE2 created the widest modeled pore aperture (6.26 Å) in the ar/R region (Fig. 7A and Supplementary Fig. S1A), whereas Ile in this position projected further into the pore than Val and narrowed the modeled pore aperture (5.41 Å). An Arg residue at position LE2 changed the pore structure even more radically (Fig. 7B, D and Supplementary Fig. S1B, D): it formed a hydrogen bond with Gly or Ala at the LE1 position (group IIa or group IIb, respectively), and resulted in greater obstruction of the pore. Furthermore, in the presence of Arg at LE2, the His residue at H2 projected into the pore notably and the combined effect narrowed the pore aperture (4.08 Å in I201R and 4.39 Å in A195G/I201R). In contrast, substitution of Ala by Gly in the A195G mutant did not lead to a significant change in pore conformation (Fig. 7C). These data indicated that the amino acid residue at LE2 in the ar/R selectivity filter affected the pore architecture as well as the pore aperture significantly.

4. Discussion

Structural, computational, and biochemical studies have revealed the ar/R region to be the key selectivity filter in aquaporins [32–

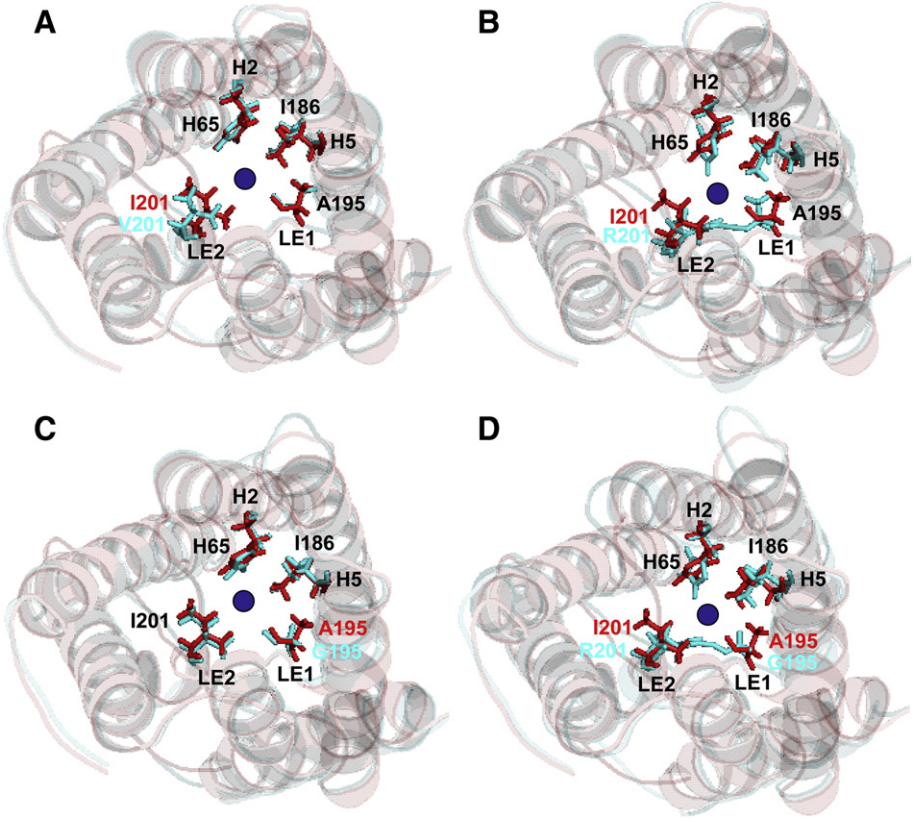

Fig. 7. Top view into the pore for homology models of wild-type TgTIP1;1 (red) superposed with those of the I201V (A), I201R (B), A195G (C) and A195G/I201R (D) mutants (cyan). The 3D models of TgTIP1;1 and its mutants were first constructed separately on the basis of homology with the experimental structure of SoPIP2;1. The 3D model of TgTIP1;1 was then superposed on that of each mutant. The residues that form the ar/R tetrad in the superposed structures are shown as sticks. The residues of TgTIP1;1 are shown in red and those of the mutants in cyan. The TM α-helices and the loops to which these residues belong are indicated. The residues at the mutation site are labeled red in wild-type TgTIP1;1 and cyan in the mutants. The center of the pore is indicated as a blue ball.

33,35,47–48]. It determines both the selectivity and rate of transport [33–34]. The amino acid composition in the ar/R selectivity filter of plant aquaporins is less conserved than that of their mammalian and microbial counterparts [5,8,31], which suggests that plant aquaporins might have more diverse transport profiles and novel physiological functions. Interestingly, TIPs exhibit the greatest degree of divergence in the ar/R region among the plant aquaporins [31], and in addition to water molecules, TIP homologs have been shown to transport different physiologically important substrates, such as NH_3/NH_4^+, urea, glycerol, and H_2O_2 [21–22,24–26,28–30]. More intriguingly, we found that TgTIP1;1 and TgTIP1;2 isolated in this study, and the TgTIP1 (Fig. 1), have an unprecedented Ile residue at LE2 in the ar/R selectivity filter. In other model plants, the corresponding residue is Val in all TIP1s, Arg in all TIP2s, TIP3s, and TIP4s, and Cys in all TIP5s [5,8,31]. We mimicked the ar/R constrictions of the TIPs from *A. thaliana* in the TgTIPs by mutating the Ile at LE2 and Ala at LE1 in the ar/R filter of TgTIP1;1 to the corresponding residues found in the group I and II AtTIPs. As a result, we found that the amino acid residue at the LE2 position played an important role in the transport selectivity profiles and transport rates of these aquaporins. While discrete reports have been done with some TIPs from *Arabidopsis* or wheat to show the transport of either ammonia [26–28], or urea [24–25] or H_2O_2 [30], molecular mechanism of transport selectivity for these substrates is not combined in these studies. Moreover, TIP-like constructs done by mutation at the ar/R region of AtPIP2;1 showed no evidence of ammonia transportation [29], and the effect of Arg at LE2 position in the ar/R selectivity filter of TaTIP2;1 was not verified although amino acid residues at H2, H5 and LE1 were substituted in three single mutants to mimic the residue at the corresponding position in an orthodox aquaporin AQP1 from bovine [26]. In our study reported herein, analysis of structure–function relationships using all the substrates used in the previous studies [24–30] explores the understanding for molecular mechanism of transport selectivity profiles of group I and II TIPs.

Heterologous expression of different TIP homologs in *P. pastoris* which is used to assay the WCA and to monitor aquaporin-mediated channel gating [16,37,49] resulted in distinct growth phenotypes and viable cell counts on the same medium under identical conditions (Figs. 4D, 5 6A and Table 3). Heterologous expression of TIPs in *P. pastoris*, coupled with the use of fast kinetics and fluorescence assays, also demonstrated that there were differences in the transport rates of water and H_2O_2 (Figs. 4B, C and 6B). However, when different concentrations of $HgCl_2$ (1.0 to 20 μM) were added to the media, growth repression with the identical concentration of $HgCl_2$ in the same medium under identical conditions was similar in the control yeast containing empty pPICZ-B and the yeasts that expressed TIP homologs (data not shown). This might be due to similar biocide effects of $HgCl_2$ on all yeast cells.

Whereas spheroplasts that expressed TgTIP1;1 and TgTIP1;2 exhibited almost the same WCA, spheroplasts that expressed the different TgTIP1;1 mutants displayed distinct rates of water transportation (Fig. 4C). However, the differences in the rate of water influx that were observed for the different TgTIP1;1 mutants in the spheroplast swelling assay were not reflected in growth rates under hyperosmotic stress (Fig. 4D). This might be due to rapid efflux of cellular water from cells expressing every TIP homolog by too short a time following hyperosmotic treatment. Similarly, differences in growth among cells that expressed the different TIP homologs could not be discerned readily following ammonium supplementation, although slightly lower growth was observed for cells that expressed the I201R mutant, which was designed to mimic all TIP3 and TIP4 homologs of *A. thaliana*. Therefore, the data presented here (Figs. 4B–D, 5) support the proposal that water and NH_3/NH_4^+ transportation might be a common function of all TIP homologs, even if the rate of transport varies between homologs. This observation is in agreement with previous reports on the functions of TIPs in *A. thaliana* and other plants [21,25–26,28–30,50]. The TgTIP1;1 mutants that were designed to mimic the ar/R selectivity filter of group I TIP homologs facilitated urea and H_2O_2 conductance, whereas the mutants that mimicked the group II TIP homologs showed no permeability to these two substrates (Figs. 5 and 6). These observed functional properties support the proposal that the transportation of urea and H_2O_2 through TIPs is TIP homolog-specific. Recently it has been shown that only group I TIP homologs in *A. thaliana* facilitate H_2O_2 conductance [30]. For solute compounds, such as urea and NH_3/NH_4^+, the first barrier is the PM and the second is the VM. Therefore, urea and NH_3/NH_4^+ enter into the cells through urea and NH_3/NH_4^+ transporters, respectively localized at the PM and then transported into vacuole [24,28,51–52].

The differences in transport selectivity profiles and transport rates that were observed can be explained by the identity of the amino acid

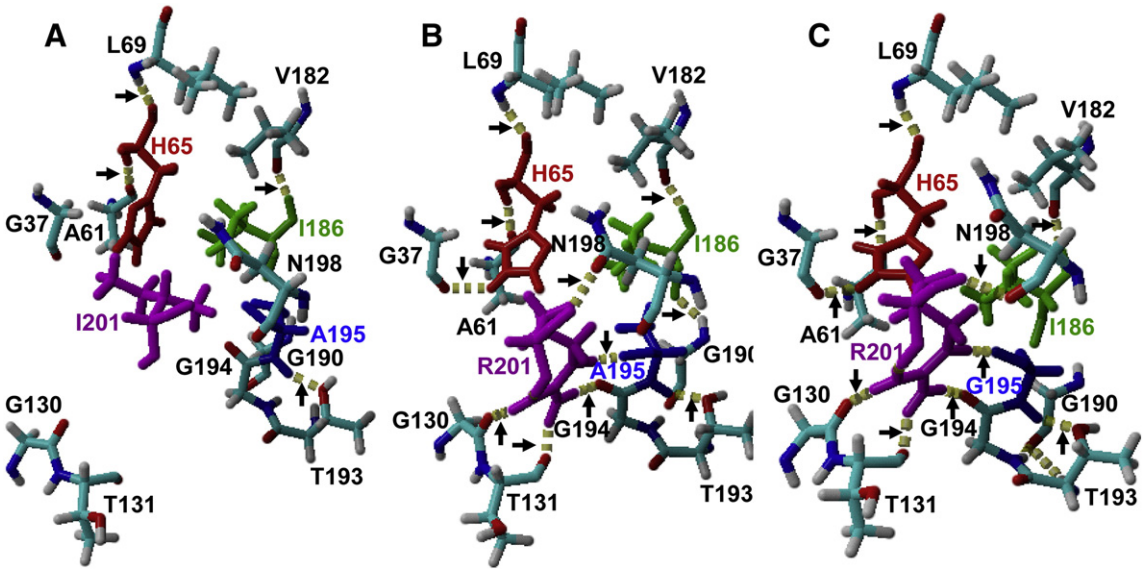

Fig. 8. Hydrogen-bonding networks of the tetrad residues in the ar/R selectivity filter of wild-type TgTIP1;1 (A) and the mutants I201R (B) and A195G/I201R (C). The homology models shown in Fig. 7 were analyzed for hydrogen-bonding networks. Hydrogen bonds are indicated by an arrow. The tetrad residues in the ar/R region are labeled with the same color: H65 (red), I186 (green), A195 (blue; A and B) and G195 (blue; C), I201 (magenta, A), and R201 (magenta, B and C).

present at LE2 in the ar/R region of the TIP homologs of groups I and II. The presence of either Ile or Val at LE2 combined with Ile at H5 and Ala at LE1 in TIP1s results in the most hydrophobic ar/R constriction site of all the TIP homologs. The greater hydrophobicity in the constriction region aids the transport of NH_3/NH_4^+ as well as that of other solutes [26]. Neither Val nor Ile at the LE2 position could form hydrogen bonding interaction with any other amino acid within the TIP molecule (Fig. 8A, I201V is not shown), but the bulkier Ile projected further into the pore, which created a narrower constriction (Figs. 3B, 7A) and reduced the pore aperture by approximately 0.8 Å. The wider pore aperture combined with the increased hydrophobic nature of the I201V construct, which was designed to mimic the TIP1 homologs in all model plants, might be responsible for the multifunctional aquaglyceroporin properties of these TIP1s [5,8,35]. The functional analysis reported here and in previous studies has established that TIP1 homologs transport a wide range of substrates [21,23–24,29–30,53].

In contrast, when hydrophilic Arg was present in the LE2 position, it formed a hydrogen bonding network with Ala (I201R; group IIb) or Gly (A195G/I201R; group IIa) at LE1, the Gly residue that is conserved in loop E (adjacent to the LE1 position) in TIPs from all model plants, and two amino acid residues (G130 and T131) in loops C (Fig. 8B, C). Due to these interactions, the flexible side chain of the Arg residue, together with that of Ala or Gly at LE1, projected into the pore (Fig. 7B, D and Supplementary Fig. S1B, D). This flexibility of the Arg residue was also observed in molecular dynamics simulations on aquaporins that were reported previously [47,54–55]. In addition, in the presence of the Arg at LE2, the hydrogen bonding networks of the His residue at H2 and the Ile at H5 become changed, and the His at H2 extends further into the pore significantly (Figs. 7B, D and 8B, C; Supplementary Fig. 1B, D). The Arg substitution at the LE2 position conferred significant changes in the structure of the pore, which resulted in the narrowest pore aperture (approximately 2.2 Å narrower in the I201R construct than for I201V). This narrow pore would be expected to restrict and selectively exclude larger solutes such as urea and H_2O_2 [35,47]. The results of functional analysis presented here correlate with this conclusion (Figs. 5–7).

The Arg residue at LE2 in the ar/R selectivity filter is conserved in the majority of aquaporins except TIP1s [5,8,31]. On the basis of the mechanism of action of the ar/R region proposed by Sui et al. [34] and homology modeling [31], TIP1s might not be expected to transport water as efficiently as those aquaporins with the conserved Arg at LE2. However, the functional analysis reported herein established that TgTIP1;1 and TgTIP1;2 had even higher WCA than TgPIP2;2 (Fig. 4B), which features an ar/R region that is highly homologous to the ar/R region of the water-selective mammalian aquaporin AQP1 [34]. This is in agreement with previous studies which elucidated that the WCA of AtTIP1;1 was at least as efficient as aquaporins with an Arg residue at the LE2 position [30,56].

The multifunctional transport activities of TgTIP1;1 and TgTIP1;2 might be associated with physiological roles in tulip flowers. The WCA might contribute to the plant water homeostasis [19] and temperature-dependent and water transport-concomitant tulip petal opening [15–16]. Despite aquaporins, plants possess transmembrane proteins that facilitate the transportation of NH_3/NH_4^+ [28] and urea [24,51]. In complement to these transporters, TgTIP1;1 and TgTIP1;2 might be required for efficient uptake of NH_3/NH_4^+ and urea during nitrogen metabolism or nutrition, and might play a role in subcellular partitioning or accumulation of NH_3/NH_4^+ and urea into vacuoles and contribute to the detoxification of these molecules [24,28,51–52]. TgTIP1;1 and TgTIP1;2 further could play a role in detoxification of H_2O_2 by translocating it into vacuoles. In tulip petals, the accumulation of H_2O_2 occurs in the late stage of petal senescence [57], in which the expression of TgTIP1;1 (ubiquitously expressed in tulip plant) and TgTIP1;2 (ubiquitously expressed except bulbs) is down-regulated (unpublished data). However, H_2O_2 transport might be involved in the signal transduction as a second messenger [58], as well as in the biosynthesis and development-related modifications of structural components of cell walls [59].

Although homology modeling can give initial insight into the transport properties of aquaporins [31], the combined use of homology modeling and functional analysis can be used to establish the selectivity profiles of aquaporins. On the basis of the results reported herein, it could be concluded that the amino acid residue at the LE2 position in the ar/R selectivity filter is a critical determinant of the transport selectivity profiles and transport rate of TIPs. The substitution of Arg at this site with a hydrophobic residue (Val/Ile) in TIP1 homologs renders them multifunctional aquaglyceroporins.

Supplementary materials related to this article can be found online at doi:10.1016/j.bbamem.2011.09.014.

Acknowledgements

A.K.A. was supported as a foreign researcher by the Invitation Fellowship Program of the Japan Society for the Promotion of Science (L09558). The work was supported in part by a grant-in-aid from the Ministry of Education, Science, Sports and Culture, Japan (No. 17.05199). The authors thank Dr. Henry Joseph Oduor Ogola (Dept. of Life Science and Biotechnology, Shimane University, Japan) for his assistance with the stopped-flow spectrophotometry analysis.

References

[1] P. Agre, M. Bonhivers, M.J. Borgnia, The aquaporins, blueprints for cellular plumbing systems, J. Biol. Chem. 273 (1998) 14659–14662.
[2] D. Gomes, A. Agasse, P. Thiebaud, S. Delrot, H. Geros, F. Chaumont, Aquaporins are multifunctional water and solute transporters highly divergent in living organisms, Biochim. Biophys. Acta 1788 (2009) 1213–1228.
[3] K. Jeyaseelan, S. Sepramaniam, A. Armugam, E.M. Wintour, Aquaporins: a promising target for drug development, Expert Opin. Ther. Targets 10 (2006) 889–909.
[4] J. Sakurai, F. Ishikawa, T. Yamaguchi, M. Uemura, M. Maeshima, Identification of 33 rice aquaporin genes and analysis of their expression and function, Plant Cell Physiol. 46 (2005) 1568–1577.
[5] A. Bansal, R. Sankararamakrishnan, Homology modeling of major intrinsic proteins in rice, maize and *Arabidopsis*: comparative analysis of transmembrane helix association and aromatic/arginine selectivity filters, BMC Struct. Biol. 7 (2007) 27.
[6] U. Johanson, M. Karlsson, I. Johansson, S. Gustavsson, S. Sjovall, L. Fraysse, A.R. Weig, P. Kjellbom, The complete set of genes encoding major intrinsic proteins in *Arabidopsis* provides a framework for a new nomenclature for major intrinsic proteins in plants, Plant Physiol. 126 (2001) 1358–1369.
[7] F. Chaumont, F. Barrieu, E. Wojcik, M.J. Chrispeels, R. Jung, Aquaporins constitute a large and highly divergent protein family in maize, Plant Physiol. 125 (2001) 1206–1215.
[8] A.B. Gupta, R. Sankararamakrishnan, Genome-wide analysis of major intrinsic proteins in the tree plant *Populus trichocarpa*: characterization of XIP subfamily of aquaporins from evolutionary perspective, BMC Plant Biol. 9 (2009) 134.
[9] C. Maurel, L. Verdoucq, D.T. Luu, V. Santoni, Plant aquaporins: membrane channels with multiple integrated functions, Annu. Rev. Plant Biol. 59 (2008) 595–624.
[10] P. Martre, R. Morillon, F. Barrieu, G.B. North, P.S. Nobel, M.J. Chrispeels, Plasma membrane aquaporins play a significant role during recovery from water deficit, Plant Physiol. 130 (2002) 2101–2110.
[11] C. Tournaire-Roux, M. Sutka, H. Javot, E. Gout, P. Gerbeau, D.T. Luu, R. Bligny, C. Maurel, Cytosolic pH regulates root water transport during anoxic stress through gating of aquaporins, Nature 425 (2003) 393–397.
[12] N. Uehlein, R. Kaldenhoff, Aquaporins and plant leaf movements, Ann. Bot. 101 (2008) 1–4.
[13] R.B. Heinen, Q. Ye, F. Chaumont, Role of aquaporins in leaf physiology, J. Exp. Bot. 60 (2009) 2971–2985.
[14] F. Chaumont, F. Barrieu, E.M. Herman, M.J. Chrispeels, Characterization of a maize tonoplast aquaporin expressed in zones of cell division and elongation, Plant Physiol. 117 (1998) 1143–1152.
[15] A.K. Azad, Y. Sawa, T. Ishikawa, H. Shibata, Phosphorylation of plasma membrane aquaporin regulates temperature-dependent opening of tulip petals, Plant Cell Physiol. 45 (2004) 608–617.
[16] A.K. Azad, M. Katsuhara, Y. Sawa, T. Ishikawa, H. Shibata, Characterization of four plasma membrane aquaporins in tulip petals: a putative homolog is regulated by phosphorylation, Plant Cell Physiol. 49 (2008) 1196–1208.
[17] H.B. Shao, L.Y. Chu, M.A. Shao, C.X. Zhao, Advances in functional regulation mechanisms of plant aquaporins: their diversity, gene expression, localization, structure and roles in plant soil–water relations (Review), Mol. Membr. Biol. 25 (2008) 179–191.

[18] H.B. Shao, L.Y. Chu, C.A. Jaleel, P. Manivannan, R. Panneerselvam, M.A. Shao, Understanding water deficit stress-induced changes in the basic metabolism of higher plants — biotechnologically and sustainably improving agriculture and the ecoenvironment in arid regions of the globe, Crit. Rev. Biotechnol. 29 (2009) 131–151.
[19] C. Hachez, F. Chaumont, Aquaporins: a family of highly regulated multifunctional channels, Adv. Exp. Med. Biol. 679 (2010) 1–17.
[20] M.M. Wudick, D.T. Luu, C. Maurel, A look inside: localization patterns and functions of intracellular plant aquaporins, New Phytol. 184 (2009) 289–302.
[21] G.W. Li, Y.H. Peng, X. Yu, M.H. Zhang, W.M. Cai, W.N. Sun, W.A. Su, Transport functions and expression analysis of vacuolar membrane aquaporins in response to various stresses in rice, J. Plant Physiol. 165 (2008) 1879–1888.
[22] P. Gerbeau, J. Guclu, P. Ripoche, C. Maurel, Aquaporin Nt-TIPa can account for the high permeability of tobacco cell vacuolar membrane to small neutral solutes, Plant J. 18 (1999) 577–587.
[23] F. Klebl, M. Wolf, N. Sauer, A defect in the yeast plasma membrane urea transporter Dur3p is complemented by CpNIP1, a Nod26-like protein from zucchini (*Cucurbita pepo* L.), and by *Arabidopsis thaliana* δ-TIP or γ-TIP, FEBS Lett. 547 (2003) 69–74.
[24] L.H. Liu, U. Ludewig, B. Gassert, W.B. Frommer, N. von Wiren, Urea transport by nitrogen-regulated tonoplast intrinsic proteins in *Arabidopsis*, Plant Physiol. 133 (2003) 1220–1228.
[25] G. Soto, K. Alleva, M.A. Mazzella, G. Amodeo, J.P. Muschietti, AtTIP1;3 and AtTIP5;1, the only highly expressed *Arabidopsis* pollen-specific aquaporins, transport water and urea, FEBS Lett. 582 (2008) 4077–4082.
[26] T.P. Jahn, A.L. Moller, T. Zeuthen, L.M. Holm, D.A. Klaerke, B. Mohsin, W. Kuhlbrandt, J.K. Schjoerring, Aquaporin homologues in plants and mammals transport ammonia, FEBS Lett. 574 (2004) 31–36.
[27] A. Bertl, R. Kaldenhoff, Function of a separate NH_3-pore in Aquaporin TIP2;2 from wheat, FEBS Lett. 581 (2007) 5413–5417.
[28] D. Loque, U. Ludewig, L. Yuan, N. von Wiren, Tonoplast intrinsic proteins AtTIP2;1 and AtTIP2;3 facilitate NH_3 transport into the vacuole, Plant Physiol. 137 (2005) 671–680.
[29] M. Dynowski, M. Mayer, O. Moran, U. Ludewig, Molecular determinants of ammonia and urea conductance in plant aquaporin homologs, FEBS Lett. 582 (2008) 2458–2462.
[30] G.P. Bienert, A.L. Moller, K.A. Kristiansen, A. Schulz, I.M. Moller, J.K. Schjoerring, T.P. Jahn, Specific aquaporins facilitate the diffusion of hydrogen peroxide across membranes, J. Biol. Chem. 282 (2007) 1183–1192.
[31] I.S. Wallace, D.M. Roberts, Homology modeling of representative subfamilies of *Arabidopsis* major intrinsic proteins. Classification based on the aromatic/arginine selectivity filter, Plant Physiol. 135 (2004) 1059–1068.
[32] E. Tajkhorshid, P. Nollert, M.O. Jensen, L.J. Miercke, J. O'Connell, R.M. Stroud, K. Schulten, Control of the selectivity of the aquaporin water channel family by global orientational tuning, Science 296 (2002) 525–530.
[33] D. Fu, A. Libson, L.J. Miercke, C. Weitzman, P. Nollert, J. Krucinski, R.M. Stroud, Structure of a glycerol-conducting channel and the basis for its selectivity, Science 290 (2000) 481–486.
[34] H. Sui, B.G. Han, J.K. Lee, P. Walian, B.K. Jap, Structural basis of water-specific transport through the AQP1 water channel, Nature 414 (2001) 872–878.
[35] I.S. Wallace, D.M. Roberts, Distinct transport selectivity of two structural subclasses of the nodulin-like intrinsic protein family of plant aquaglyceroporin channels, Biochemistry 44 (2005) 16826–16834.
[36] M.J. Daniels, M. Yeager, Phosphorylation of aquaporin PvTIP3;1 defined by mass spectrometry and molecular modeling, Biochemistry 44 (2005) 14443–14454.
[37] A.K. Azad, Y. Sawa, T. Ishikawa, H. Shibata, Heterologous expression of tulip petal plasma membrane aquaporins in *Pichia pastoris* for water channel analysis, Appl. Environ. Microbiol. 75 (2009) 2792–2797.
[38] M.J. Tamas, K. Luyten, F.C. Sutherland, A. Hernandez, J. Albertyn, H. Valadi, H. Li, B.A. Prior, S.G. Kilian, J. Ramos, L. Gustafsson, J.M. Thevelein, S. Hohmann, Fps1p controls the accumulation and release of the compatible solute glycerol in yeast osmoregulation, Mol. Microbiol. 31 (1999) 1087–1104.
[39] Y. Nakanishi, T. Saijo, Y. Wada, M. Maeshima, Mutagenic analysis of functional residues in putative substrate-binding site and acidic domains of vacuolar H^+-pyrophosphatase, J. Biol. Chem. 276 (2001) 7654–7660.
[40] D.F. Savage, R.M. Stroud, Structural basis of aquaporin inhibition by mercury, J. Mol. Biol. 368 (2007) 607–617.
[41] D. Kozono, X. Ding, I. Iwasaki, X. Meng, Y. Kamagata, P. Agre, Y. Kitagawa, Functional expression and characterization of an archaeal aquaporin. AqpM from *Methanothermobacter marburgensis*, J. Biol. Chem. 278 (2003) 10649–10656.
[42] G. Calamita, D. Ferri, P. Gena, G.E. Liquori, A. Cavalier, D. Thomas, M. Svelto, The inner mitochondrial membrane has aquaporin-8 water channels and is highly permeable to water, J. Biol. Chem. 280 (2005) 17149–17153.
[43] K. Liu, H. Nagase, C.G. Huang, G. Calamita, P. Agre, Purification and functional characterization of aquaporin-8, Biol. Cell 98 (2006) 153–161.
[44] S. Tornroth-Horsefield, Y. Wang, K. Hedfalk, U. Johanson, M. Karlsson, E. Tajkhorshid, R. Neutze, P. Kjellbom, Structural mechanism of plant aquaporin gating, Nature 439 (2006) 688–694.
[45] P.A. Balk, A.D. de Boer, Rapid stalk elongation in tulip (*Tulipa gesneriana* L. cv. Apeldoorn) and the combined action of cold-induced invertase and the water-channel protein γTIP, Planta 209 (1999) 346–354.
[46] G. Fischer, U. Kosinska-Eriksson, C. Aponte-Santamaria, M. Palmgren, C. Geijer, K. Hedfalk, S. Hohmann, B.L. de Groot, R. Neutze, K. Lindkvist-Petersson, Crystal structure of a yeast aquaporin at 1.15 angstrom reveals a novel gating mechanism, PLoS Biol. 7 (2009) e1000130.
[47] M. Dynowski, G. Schaaf, D. Loque, O. Moran, U. Ludewig, Plant plasma membrane water channels conduct the signalling molecule H_2O_2, Biochem. J. 414 (2008) 53–61.
[48] R.M. Stroud, D. Savage, L.J. Miercke, J.K. Lee, S. Khademi, W. Harries, Selectivity and conductance among the glycerol and water conducting aquaporin family of channels, FEBS Lett. 555 (2003) 79–84.
[49] M.J. Daniels, M.R. Wood, M. Yeager, In vivo functional assay of a recombinant aquaporin in *Pichia pastoris*, Appl. Environ. Microbiol. 72 (2006) 1507–1514.
[50] L.M. Holm, T.P. Jahn, A.L. Moller, J.K. Schjoerring, D. Ferri, D.A. Klaerke, T. Zeuthen, NH_3 and NH_4^+ permeability in aquaporin-expressing *Xenopus* oocytes, Pflugers Arch. 450 (2005) 415–428.
[51] S. Kojima, A. Bohner, N. von Wiren, Molecular mechanisms of urea transport in plants, J. Membr. Biol. 212 (2006) 83–91.
[52] E. Martinoia, M. Maeshima, H.E. Neuhaus, Vacuolar transporters and their essential role in plant metabolism, J. Exp. Bot. 58 (2007) 83–102.
[53] P.H. Nord-Larsen, T. Kichey, T.P. Jahn, C.S. Jensen, K.K. Nielsen, J.N. Hegelund, J.K. Schjoerring, Cloning, characterization and expression analysis of tonoplast intrinsic proteins and glutamine synthetase in ryegrass (*Lolium perenne* L.), Plant Cell Rep. 28 (2009) 1549–1562.
[54] B.G. Han, A.B. Guliaev, P.J. Walian, B.K. Jap, Water transport in AQP0 aquaporin: molecular dynamics studies, J. Mol. Biol. 360 (2006) 285–296.
[55] F. Zhu, E. Tajkhorshid, K. Schulten, Theory and simulation of water permeation in aquaporin-1, Biophys. J. 86 (2004) 50–57.
[56] C. Maurel, J. Reizer, J.I. Schroeder, M.J. Chrispeels, The vacuolar membrane protein γ-TIP creates water specific channels in *Xenopus* oocytes, EMBO J. 12 (1993) 2241–2247.
[57] A.K. Azad, T. Ishikawa, Y. Sawa, H. Shibata, Intracellular energy depletion triggers programmed cell death during petal senescence in tulip, J. Exp. Bot. 59 (2008) 2085–2095.
[58] S.M. McInnis, R. Desikan, J.T. Hancock, S.J. Hiscock, Production of reactive oxygen species and reactive nitrogen species by angiosperm stigmas and pollen: potential signalling crosstalk? New Phytol. 172 (2006) 221–228.
[59] A.R. Ros Barcelo, L.V. Gomes-Ros, C. Gabaldon, M. Lopez-Serrano, F. Pomar, J.S. Carrion, M.A. Pedreno, Basic peroxidase: the gateway for lignin evolution? Phytochem. Rev. 3 (2004) 61–78.
[60] M.J. Daniels, F. Chaumont, T.E. Mirkov, M.J. Chrispeels, Characterization of a new vacuolar membrane aquaporin sensitive to mercury at a unique site, Plant Cell 8 (1996) 587–599.
[61] K. Tamura, J. Dudley, M. Nei, S. Kumar, MEGA4: molecular evolutionary genetics analysis (MEGA) software version 4.0, Mol. Biol. Evol. 24 (2007) 1596–1599.